Supporting Information

Table S1 Basic physicochemical properties of four FQs and two molecular probe.

Adsorbate	Structure	Log K_{ow} [a)]	pK_a [b)]
Ciprofloxacin CIP	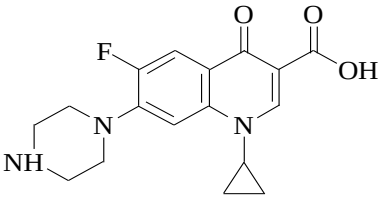	0.28	pK_{a1} = 6.14 pK_{a2} = 8.85
Norfloxacin NOR	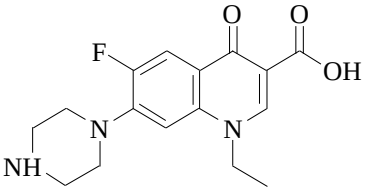	0.46	pK_{a1} = 6.27 pK_{a2} = 8.71
Enrofloxacin ENR	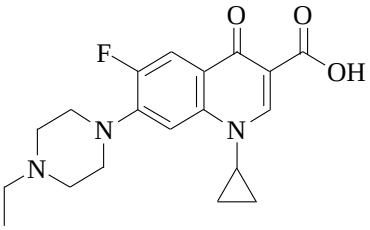	0.7	pK_{a1} = 6.20 pK_{a2} = 8.13
Ofloxacin OFL	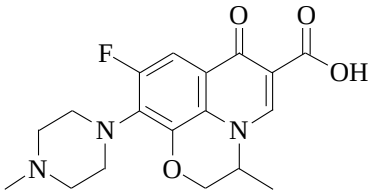	–0.39	pK_{a1}= 5.98 pK_{a2}= 8.00
1-(2-fluorophenyl) piperazine FPP	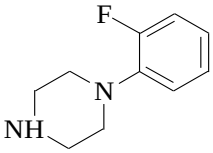		pK_{a1} = 4.49 pK_{a2} = 8.63
Flumequine FLU	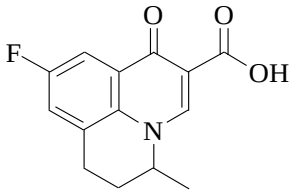		pK_a = 6.29

Notes: a) Log K_{ow} values were obtained from Jiang et al. (2016); b) pK_a values were obtained from Van Doorslaer et al. (2014).

Table S2 Fitting parameters of the pseudo-first-order and pseudo-second-order kinetic models for CMC and various CMC-CG aerogels in adsorption of CIP at the initial CIP concentration of 0.2 mmol/L.

Aerogel	$q_{m,exp}$ (mmol/g)	Pseudo-first-order kinetics			Pseudo-second-order kinetics		
		q_e (mmol/g)	k_1 (min^{-1})	R^2	q_e (mmol/g)	k_2 (g/(mmol·min))	R^2
CMC	0.682	0.656	0.418	0.983	0.705	0.673	0.993
CMC-CG1	0.706	0.674	0.406	0.977	0.722	0.652	0.991
CMC-CG2	0.800	0.767	0.465	0.971	0.821	0.688	0.987
CMC-CG3	0.748	0.678	0.525	0.956	0.727	0.894	0.988
CMC-CG4	0.818	0.803	0.342	0.990	0.861	0.414	0.991
CMC-CG5	0.856	0.806	0.308	0.980	0.860	0.370	0.994

Table S3 Fitting parameters of the Langmuir and Freundlich isothermal models for CMC and CMC-CG aerogels in adsorption of CIP.

Aerogel	$q_{max,exp}$ (mmol/g)	Langmuir model			Freundlich model		
		q_m (mmol/g)	K_L (L/mmol)	R^2	K_F	n	R^2
CMC	0.788	1.023	16.623	0.995	1.682	2.211	0.919
CMC-CG1	0.893	1.254	12.736	0.999	2.158	1.947	0.969
CMC-CG2	0.967	1.271	18.999	0.992	2.259	2.175	0.907
CMC-CG3	0.902	1.162	18.711	0.992	2.002	2.216	0.911
CMC-CG4	0.995	1.293	20.020	0.989	2.320	2.206	0.898
CMC-CG5	1.123	1.502	20.268	0.989	2.900	2.095	0.905

Table S4 Fitting parameters of adsorption thermodynamics for CMC and CMC-CG2 aerogels in adsorption of CIP.

Aerogel	Temperature (K)	K_L (L/mmol)	ΔG^0 (kJ/mol)	ΔH^0 (kJ/mol)	ΔS^0 (kJ/(mol·K))
CMC	298	16.623	–34.031	–21.805	0.041
	308	12.591	–34.461		
	318	9.559	–34.852		
CMC-CG2	298	18.999	–34.362	–19.586	0.05
	308	14.778	–34.872		
	318	11.556	–35.354		

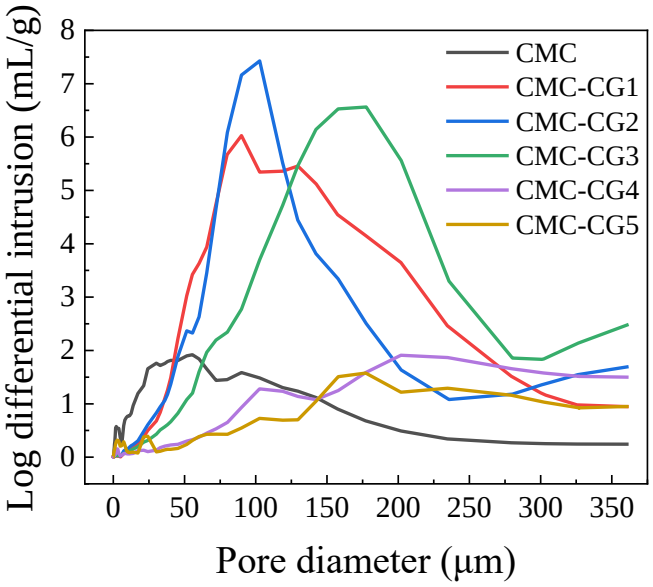

Fig. S1 The pore size distribution of various CMC-based aerogels.

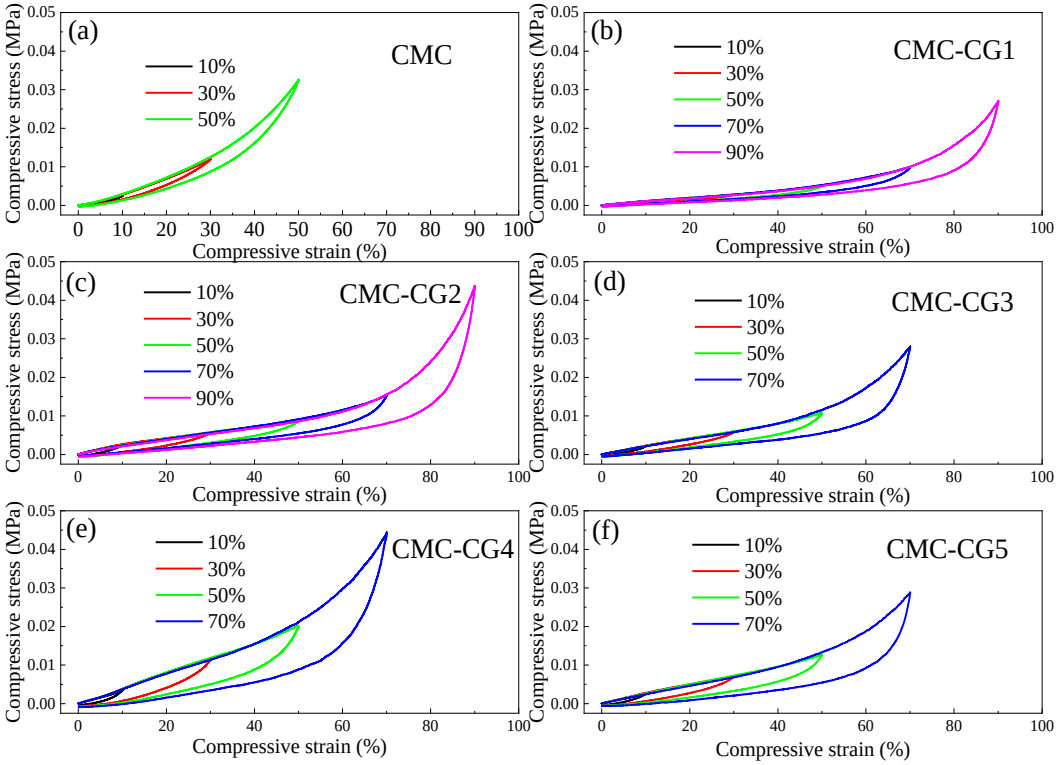

Fig. S2 The compressive strength of various CMC-based aerogels. (a) CMC; (b) CMC-CG1; (c) CMC-CG2; (d) CMC-CG3; (e) CMC-CG4; and (f) CMC-CG5, respectively.

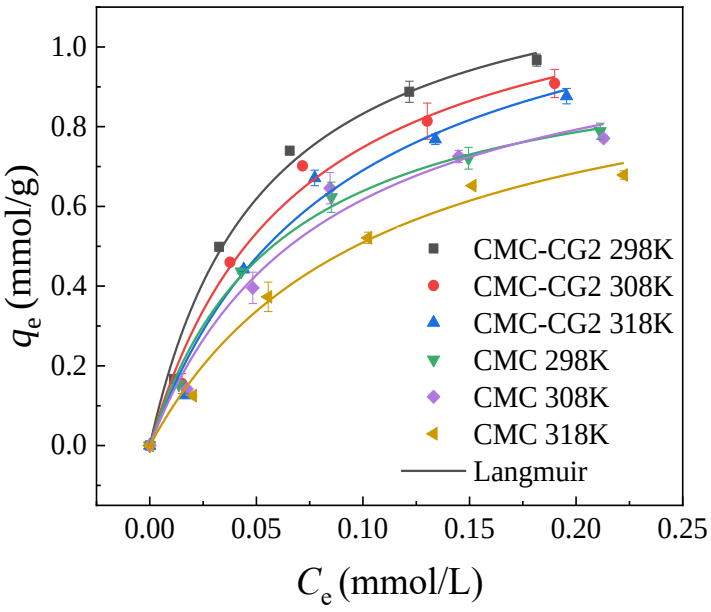

Fig. S3 Adsorption isotherms of CMC and CMC-CG2 aerogels for CIP adsorption at different temperatures and the initial pH of 5.0.

Text S1 Characterization of aerogels

The CMC-CG aerogel before and after adsorption was analyzed by a Fourier transform infrared spectrometry (TENSOR 27, Bruker Co., Germany) in the wavenumber range of 500–4000 cm^{-1} and an X-ray photoelectron spectroscopy (PHI5000 VersaProbe, ULVAC PHI, Japan), respectively. The thermogravimetric analysis (TGA) was carried from room temperature to 800℃ with a heating rate of 10.0℃/min under 50.0 mL/min of nitrogen flow by a thermogravimetric analyzer (TG-DSC STA 449 F3, NETZSCH, Germany). The surface morphology of aerogels was observed under a scanning electron microscope (SEM) (TM4000Plus, Hitach, Japan). The specific surface area and pore volume of aerogels were determined via a nitrogen adsorption-desorption and Brunauer-Emmett-Teller (BET) method by a surface area analyzer (ASAP2020, Micromeritics, USA) and a high-performance automatic mercury porosimeter (AutoPore Iv 9510, Micromeritics, USA), respectively. The mechanical property of the aerogels was tested by using a universal testing machine (5944, Instron, USA). The swelling ratio (*SR*) of the aerogels were estimated by the weighting method (Yu et al., 2019). A known amount of aerogel was immersed into a large excess of water or 0.1 mol/L of NaCl aqueous solution at room temperature to reach swelling equilibrium, respectively. *SR* was calculated as follows (Eq. (S1)):

$$SR = \frac{W_1 - W_0}{W_0} \times 100\% \quad , \qquad \text{(S1)}$$

where W_0 and W_1 (g) are the weight of dry and fully swollen aerogel, respectively.

Text S2 Batch adsorption experiments

pH effect

Batch adsorption experiments were conducted by mixing 10.0 mg of the aerogel in a 60 mL of pollutant aqueous solution. The pH effect on the adsorption of various FQs (CIP, NOR, ENR, and OFL) and two molecular probes (FPP and FLU), of which structures are presented in Supporting Information Table S1 was studied at the initial pollutant concentration of 0.2 mmol/L and pH ranging from 2.0 to 10.0 adjusted by 0.1 mol/L HCl and 0.1 mol/L NaOH aqueous solutions. Then, the mixtures were shaken in a thermostatic oscillator at 180 r/min and 25℃ for 24.0 h to reach equilibrium adsorption, and the solution sample was filtered by a 0.45 μm filter (PTFE, Agilent, USA). The concentrations of FQs were analyzed by using an Agilent HPLC Series 1200 instrument (USA). The FQs uptake of the aerogel was calculated according to the following expression (Eq. (S2)):

$$q_e = \frac{(C_0 - C_e)\ V}{m} \quad , \qquad \text{(S2)}$$

where C_0 and C_e (mg/L) are the initial and equilibrium pollutant concentrations, respectively; V (L) is the volume of working solution; m (g) is the mass of aerogel.

Adsorption kinetics, isotherms, and thermodynamics

The effect of contact time on the adsorption capacity was proceeded to investigate the adsorption kinetics, by varying the contact time up to 24.0 h at the initial pH of 5.0 with the initial CIP concentration of 0.2 mmol/L. The adsorption capacity of CIP at time (t_i) was calculated based on Eq. (S3):

$$q(t_i) = \frac{(C_0 - C_{t_i})V_0 - \sum_2^{i-1} C_{t_{i-1}} V}{m} \quad , \qquad \text{(S3)}$$

where C_0 and C_{t_i} (mmol/L) represent the initial CIP concentrations and CIP concentrations at t_i, respectively. V_0 and V are the volume of the CIP solution and that of the sample solution taken out every time for CIP concentrations analysis, respectively. m (g) is the dried weight of the aerogel.

Then, the adsorption isotherms were investigated by varying the initial CIP concentrations from 0.04 mmol/L to 0.36 mmol/L at initial pH of 5.0 in 24.0 h under varied temperatures, that is, 298K, 308K, and 318K, respectively. Accordingly, the adsorption thermodynamics was further studied. The residual CIP concentrations were determined by HPLC (1200, Agilent, USA) and the CIP uptakes under various conditions were calculated by Eq. (S2) as described in detail in **Section of pH effect**.

The detailed analysis methods including theoretic kinetic and isothermal models and thermodynamic equations are described in **Supporting Information Text S3**.

Effects of coexisting substances

The influences of the coexisting cations, anions and a natural organic matter (HA) on the CIP uptakes of CMC-CG2 were performed, respectively, at the initial CIP concentration of 0.2 mmol/L and 25℃ under the initial pH of 5.0. Four measured cations were based on NaCl, $CaCl_2$, $CuCl_2$, and $FeCl_3$; while three anions were NaCl, Na_2SO_4, and Na_3PO_4. The residual CIP concentrations were tested by HPLC and the CIP uptakes under various conditions were calculated by Eq. (S2) as described in detail in **Section of pH effect**.

Reusability

The reusability of the aerogel after saturated adsorption of CIP was also investigated. The aerogel was regenerated by using 60.0 mL 0.2 mol/L NaCl aqueous solution at room temperature for 24 hours. The desorbed CMC-CG2 aerogel was separated from solution using tweezer, washed with distilled water, and directly reused in the next adsorption experiment after squeezed out the water. The adsorption-desorption experiment was carried out five cycles.

Moreover, another method for reuse of the aerogel after saturated adsorption was tried, that is, the aerogel was used as a new adsorbent to directly adsorb Cu^{2+} ions in water. The stability of the CIP-loaded aerogel was first tested at various pH levels. The aerogel after saturated adsorption was washed with distilled water and immerged in deionized water at different initial pHs under continuous stirring at 25℃ for 24.0 h. The initial and the residual CIP concentrations in the immerged solutions were analyzed by HPLC to estimate the desorption percentage and investigate the stability of the CIP-loaded aerogels. Then CIP-loaded aerogels were immerged into 0.1 mmol/L Cu^{2+} aqueous solutions with different initial pHs ranged from 2.0 to 6.0 at 25℃ in 24.0 h for direct adsorption of Cu^{2+} ions. The residual Cu^{2+} concentrations in solutions were analyzed by an inductively coupled plasma mass spectrometer (ICP-MS) (iCAP Qc, Thermo Fisher Scientific, Germany), and the Cu^{2+} uptake was calculated by Eq. (S2). The adsorption of Cu^{2+} ions has been also compared by the same aerogel without CIP adsorption.

All adsorption experiments were tried in triplicate, and the final results were the average of three runs with a relative error of less than 5%.

Text S3 Description of adsorption kinetics models, adsorption isothermal models and adsorption thermodynamics

Adsorption kinetics

In order to investigate the kinetic mechanism of adsorption, pseudo-first-order (Ho and McKay, 1998) and pseudo-second-order (Lagergren, 1989) models were used to evaluate the results.

The pseudo-first-order and pseudo-second-order models (Lagergren, 1989; Ho and McKay, 1998) are written as Eqs. (S4) and (S5), respectively:

$$ln(q_e - q_t) = lnq_e - k_1 t \quad , \qquad (S4)$$

$$\frac{t}{q_t} = \frac{1}{k_2 q_e^2} + \frac{t}{q_e} \quad , \qquad \text{(S5)}$$

where q_e and q_t (mmol/g) represent the amount of pollutants adsorbed onto adsorbent at equilibrium and at time t (min) respectively. k_1 (min^{-1}) and k_2 (g/(mmol·min)) are the rate constants of pseudo-first-order and pseudo-second-order models, respectively.

Adsorption isothermal models

Langmuir and Freundlich equations (Freundlich, 1906; Langmuir, 1918) were used to simulate the adsorption isotherms. Langmuir model (Langmuir, 1918) can be expressed as follows (Eq. (S6)):

$$q_e = \frac{q_m \cdot K_L \cdot C_e}{1 + K_L \cdot C_e} \quad , \qquad \text{(S6)}$$

where q_e (mmol/g) and C_e (mmol/L) represent concentration and uptake of pollutants at equilibrium, respectively. q_e (mmol/g) is the saturation adsorption capacity, representing the maximum pollutant's uptake, and K_L (L/mmol) is the Langmuir adsorption constant.

Freundlich model (Freundlich, 1906) is another frequently applied isotherm model which equation is expressed as follows (Eq. (S7)):

$$q_e = K_F \cdot C_e^{1/n} \quad , \qquad \text{(S7)}$$

where K_F is the Freundlich isotherm constant, and n (dimensionless) is the heterogeneity factor, respectively.

Adsorption Thermodynamics

Enthalpy change (ΔH^0, kJ/mol), entropy change (ΔS^0, kJ/(mol·K)) and Gibbs free energy change (ΔG^0, kJ/mol) were calculated by the following formula (Eqs. (S8)–(S10)) (Tran et al., 2017):

$$\Delta G^0 = -RT \cdot \ln K_c, \qquad \text{(S8)}$$

$$\Delta G^0 = \Delta H^0 - T \cdot \Delta S^0, \qquad \text{(S9)}$$

$$K_c = 55.5 \times 1000 \times K_L, \qquad \text{(S10)}$$

where R is the universal gas constant approximately 8.3144 J/(mol·K) and T is the absolute temperature in Kelvin. K_c is the equilibrium constant and is dimensionless. K_L (L/mmol) is the Langmuir adsorption constant.

References

Freundlich H M F (1906). Over the adsorption in solution. Journal of Physical Chemistry, 57: 385–470

Ho Y S, McKay G (1998). Sorption of dye from aqueous solution by peat. Chemical Engineering Journal, 70(2): 115–124

Jiang C, Ji Y, Shi Y, Chen J, Cai T (2016). Sulfate radical-based oxidation of fluoroquinolone antibiotics: Kinetics, mechanisms and effects of natural water matrices. Water Research, 106: 507–517

Lagergren S (1989). About the theory of so-called sorption of soluble substances. Kungliga Svenska Vetenskapsakademiens Handlingar, 24: 1–39

Langmuir I (1918). The adsorption of gases on plane surfaces of glass, mica and platinum. Journal of the American Chemical Society, 40(9): 1361–1403

Tran H N, You S J, Hosseini-Bandegharaei A, Chao H P (2017). Mistakes and inconsistencies regarding adsorption of contaminants from aqueous solutions: A critical review. Water Research, 120: 88–116

Van Doorslaer X, Dewulf J, Van Langenhove H, Demeestere K (2014). Fluoroquinolone antibiotics: an emerging class of environmental micropollutants. Science of the Total Environment, 500–501: 250–269

Yu F, Cui T, Yang C, Dai X, Ma J (2019). κ-Carrageenan/Sodium alginate double-network hydrogel with enhanced mechanical properties, anti-swelling, and adsorption capacity. Chemosphere, 237: 124417